JCI insight

S100a4-Cre-mediated deletion of *Patched1* causes hypogonadotropic hypogonadism: role of pituitary hematopoietic cells in endocrine regulation

Yi Athena Ren, … , Tatiana Fiordelisio Coll, JoAnne S. Richards

JCI Insight. 2019. https://doi.org/10.1172/jci.insight.126325.

Research In-Press Preview **Endocrinology** **Reproductive biology**

Hormones produced by the anterior pituitary gland regulate an array of important physiological functions, but pituitary hormone disorders are not fully understood. Herein we report that genetically-engineered mice with deletion of the hedgehog signaling receptor *Patched1* by *S100a4* promoter-driven Cre recombinase (*S100a4-Cre;Ptch1*$^{fl/fl}$ mutants) exhibit adult-onset hypogonadotropic hypogonadism and multiple pituitary hormone disorders. During the transition from puberty to adult, *S100a4-Cre;Ptch1*$^{fl/fl}$ mice of both sexes develop hypogonadism coupled with reduced gonadotropin levels. Their pituitary glands also display severe structural and functional abnormalities, as revealed by transmission electron microscopy and expression of key genes regulating pituitary endocrine functions. *S100a4-Cre* activity in the anterior pituitary gland is restricted to CD45^{+} cells of hematopoietic origin, including folliculo-stellate cells and other immune cell types, causing sex-specific changes in the expression of genes regulating the local microenvironment of the anterior pituitary. These findings provide in vivo evidence for the importance of pituitary hematopoietic cells in regulating fertility and endocrine function, in particular during sexual maturation and likely through sexually dimorphic mechanisms. These findings support a previously unrecognized role of hematopoietic cells in causing hypogonadotropic hypogonadism and provide inroads into the molecular and cellular basis for pituitary hormone disorders in humans.

Title: *S100a4-Cre*-mediated deletion of *Patched1* causes hypogonadotropic hypogonadism: role of pituitary hematopoietic cells in endocrine regulation.

Abstract:

Hormones produced by the anterior pituitary gland regulate an array of important physiological functions, but pituitary hormone disorders are not fully understood. Herein we report that genetically-engineered mice with deletion of the hedgehog signaling receptor *Patched1* by *S100a4* promoter-driven Cre recombinase (*S100a4-Cre;Ptch1*$^{fl/fl}$ mutants) exhibit adult-onset hypogonadotropic hypogonadism and multiple pituitary hormone disorders. During the transition from puberty to adult, *S100a4-Cre;Ptch1*$^{fl/fl}$ mice of both sexes develop hypogonadism coupled with reduced gonadotropin levels. Their pituitary glands also display severe structural and functional abnormalities, as revealed by transmission electron microscopy and expression of key genes regulating pituitary endocrine functions. *S100a4-Cre* activity in the anterior pituitary gland is restricted to CD45^{+} cells of hematopoietic origin, including folliculo-stellate cells and other immune cell types, causing sex-specific changes in the expression of genes regulating the local microenvironment of the anterior pituitary. These findings provide *in vivo* evidence for the importance of pituitary hematopoietic cells in regulating fertility and endocrine function, in particular during sexual maturation and likely through sexually dimorphic mechanisms. These findings support a previously unrecognized role of hematopoietic cells in causing hypogonadotropic hypogonadism and provide inroads into the molecular and cellular basis for pituitary hormone disorders in humans.

Authors: Yi Athena Ren[1*], Teresa Monkkonen[2], Michael T. Lewis[1,3,4], Daniel J. Bernard[5], Helen C. Christian[6], Carolina J. Jorgez[7], Joshua A. Moore[7], John D. Landua[1,3,4], Haelee M. Chin[8], Weiqin Chen[9], Swarnima Singh[1,4], Ik Sun Kim[1,4], Xiang H.-F. Zhang[1,4], Yan Xia[1], Kevin J. Phillips[1], Harry MacKay[10], Robert A Waterland[10], M. Cecilia Ljungberg[11,12], Pradip Saha[1], Sean M. Hartig[1], Tatiana Fiordelisio Coll[13,14], and JoAnne S. Richards[1]

[1]Department of Molecular and Cellular Biology, Baylor College of Medicine, Houston, Texas 77030, USA; [2]Department of Pathology, University of California, San Francisco, CA 94143, USA; [3]Department of Radiology, [4]Lester and Sue Smith Breast Center, Baylor College of Medicine, Houston, Texas 77030, USA; [5]Department of Pharmacology and Therapeutics, McGill University, Montreal, Quebec H3G 1Y6 Canada; [6]Department of Physiology, Anatomy and Genetics, University of Oxford, Oxford, OX1 3QX, UK; [7]Department of Urology, Baylor College of Medicine, Houston, Texas 77030, USA; [8]Department of Biology, Rice University, Houston, Texas 77005, USA; [9]Department of Physiology, Augusta University, Augusta, Georgia 30912, USA; [10]USDA/ARS Children's Nutrition Research Center, Houston, Texas 77030, USA; [11]Department of Pediatrics, Baylor College of Medicine, Houston, Texas 77030, USA; [12]Jan and Dan Duncan Neurological Research Center at Texas Children's Hospital, Houston, Texas 77030, USA; [13]Institut de Génomique Fonctionnelle, Centre National de la Recherche Scientifique, Institut National de la Santé et de la Recherche Médicale, University of Montpellier, F-34094 Montpellier, France; and [14]Laboratorio de Neuroendocrinología Comparada, Departamento de Ecología y Recursos Naturales, Biología, Facultad de Ciencias, Universidad Nacional Autónoma de México, Ciudad Universitaria, 04510 México City, Distrito Federal, México

*Correspondence Information:
Yi Athena Ren, PhD
Department of Animal Science, Cornell University
203 Morrison Hall, 507 Tower Rd,

Ithaca, NY, 14853
Email: yi.a.ren@cornell.edu
Phone: 607.255.2255
Fax: 607.255.9829

MTL is a Founder of, and Limited Partner in StemMed Ltd, and a Manager in StemMed Holdings, its general partner. He is also a Founder of Tvardi Therapeutics and holds an equity stake. All other authors have declared that no conflict of interest exists.

Introduction

The hedgehog (HH) signaling pathway regulates both the development and function of endocrine organs and reproductive tissues, including mammary glands, gonads, and the pituitary gland. In mammary glands, activated canonical HH signaling impacts stromal/fibroblast cell function and branching of the mammary ducts (1). In the gonads, it regulates Leydig cell differentiation in the testis and theca cell recruitment and differentiation as well as vascularization in the ovary (2-6). HH signaling is also a key regulator of embryonic pituitary development (7). Human patients with disrupted HH signaling suffer from a wide range of pituitary pathologies including agenesis, combined pituitary hormone deficiency and adenocarcinoma (7-10). The anterior pituitary gland is a master endocrine organ that controls a myriad of important physiological functions via orchestrated hormone release by five specialized endocrine cell types: thyrotropes produce thyroid stimulating hormone (TSH) to regulate metabolism; corticotropes produce adrenocorticotropin (ACTH) to regulate stress response; somatotropes produce growth hormone (GH) to regulate body growth; lactotropes produce prolactin (PRL) to regulate lactation; and gonadotropes produce follicle-stimulating hormones (FSH) and luteinizing hormones (LH) to regulate reproductive functions. While signals from the hypothalamus are key drivers of pituitary development and function, the importance of an intra-pituitary regulatory network is also emerging (11-15). Given this functional and cellular complexity, it is not surprising that despite considerable effort in identifying the genetic and non-genetic factors causing pituitary hormone disorders, such as acquired hypogonadotropic hypogonadism, our understanding remains limited.

In mammals, signaling ligands Sonic, Indian, and Desert HH (SHH, IHH and DHH) are secreted morphogens that undergo multiple modifications to enable their short- or long-distance dispersion from the source cells (16). These ligands bind to the transmembrane receptors PATCHED1/2 (PTCH1/2), as well as 'co-receptors cell adhesion molecule-related/down-regulated by oncogenes' (CDON) and 'growth-arrest-specific 1' (GAS1) to elicit downstream

effects (17, 18). HH ligand binding to PTCH1 activates another transmembrane receptor, Smoothened (SMO). Signaling downstream of SMO is mediated by the 'GLI-Kruppel family member' (GLI) transcription factors 1, 2 and 3. Downstream transcriptional targets of the signaling activity include *Gli1* and *Ptch1* themselves, thus forming a self-regulatory feedback loop. While HH signaling plays a key role in the embryonic development of the gonads and pituitary, precisely what cell types are targeted by HH signaling at this early stage, as well as whether and how HH signaling may also regulate functions of the gonads and pituitary in adult life, remain to be defined (16, 19).

S100 calcium binding protein A4 (S100A4), also known as fibroblast specific protein-1 (FSP1), is expressed in distinct stromal-interstitial cell types, such as fibroblasts, immune cells and tumor cells (20, 21). To investigate whether stromal-interstitial PTCH1 plays a role in regulating endocrine tissue development and function, *S100a4-Cre* mice were used to disrupt the *Ptch1* gene by crossing them with *Ptch1*$^{fl/fl}$ mice (22). These mice displayed stunted mammary ducts which were partially rescued by transplantation to a wild-type host (22), implicating a defect in the hypothalamic-pituitary-gonadal (HPG) axis caused by the deletion of *Ptch1* in stromal cell types. Indeed, fertility was reduced and estrous cycle was absent in these mutant mice, suggesting impaired ovarian function. Previous studies also showed that stunted mammary duct phenotypes of mice homozygous for a hypomorphic allele of *Ptch1* (*Ptch1*^{mes}) could be rescued by isograft of a wild-type pituitary, suggesting that *Ptch1* is required for normal pituitary function (23). Therefore, we investigated whether PTCH1 in ovarian and pituitary stromal-interstitial cells is essential for the development and function of these two organs and, consequently, for female fertility.

Surprisingly, we found not only ovarian dysfunction but also testicular dysfunction in the *S100a4-Cre;Ptch1*$^{fl/fl}$ mice. Moreover, we found that the majority of S100A4-expressing cells in the gonads are not fibroblasts, but CD45^{+} (official gene name: protein tyrosine phosphatase receptor type C; abbreviated as *Ptprc*) hematopoietic cells. *S100a4-Cre;Ptch1*$^{fl/fl}$ mutant mice also

exhibit severe defects in pituitary endocrine functions, including hypogonadotropic hypogonadism and multiple hormone disorders, which are not observed until the transition from puberty to adulthood. Integrated cellular and molecular analyses provide evidence that $CD45^{+}$ cells in the pituitary of the *S100a4-Cre;Ptch1*$^{fl/fl}$ mice, including folliculo-stellate (FS) cells, exert abnormal functions that underlie disorders in pituitary endocrine cells. Together, our data demonstrate that dysregulation of HH signaling activity in pituitary hematopoietic cells impacts the sexual maturation of the pituitary gland and subsequent endocrine function during adult life.

Results

Genetic ablation of Ptch1 with S100a4-Cre leads to hypogonadism in adult female and male mice. Following previous observations that female *S100a4-Cre;Ptch1$^{fl/fl}$* mice are infertile and exhibit mammary gland defects similar to those of estrogen receptor knockout mice (22), we investigated the cause of infertility and ovarian function in these mice. At 8 weeks of age, the ovaries and uteri of *S100a4-Cre;Ptch1$^{fl/fl}$* females were severely hypotrophic (Figure. 1A and Table 1). Histological analyses of hematoxylin and eosin (H&E) stained ovarian tissue sections showed corpora lutea (CL) and follicles at various stages of development in wild-type controls (*Ptch1$^{fl/fl}$*) and heterozygous mutants (*S100a4-Cre;Ptch1$^{fl/fl}$*), whereas no CL were observed in *S100a4-Cre;Ptch1$^{fl/fl}$* homozygous mutants, and their follicles rarely grew beyond pre-antral stage (Figure 1B). In addition, degenerating oocytes (Figure 1B, black arrows) appeared to be present more frequently in the ovaries of homozygous mutant mice compared to wild-type control and heterozygous mutant mice. Consistent with these histological observations, mRNA expression analyses by quantitative real-time PCR (qPCR) revealed reduced expression of critical genes involved in steroidogenesis, including cytochrome P450, family 17, subfamily a, polypeptide 1 (*Cyp17a1*), cytochrome P450, family 11, subfamily a, polypeptide 1 (*Cyp11a1*), and luteinizing hormone/choriogonadotropin receptor (*Lhcgr*) (Figure 1C), indicating impaired ovarian function in homozygous mutant mice. Levels of mRNA for secreted frizzled-related protein 4 (*Sfrp4*) was reduced in the homozygous mutants relative to heterozygous mutants but not wild-type controls. In contrast, ovarian expression of anti-Müllerian hormone (*Amh*), a marker of pre-antral follicles, was increased in homozygous mutant mice, consistent with their histological enrichment of this follicle population. Levels of mRNA for follicle stimulating hormone receptor (*Fshr*) and androgen receptor (*Ar*) were normal in the homozygous mutants, suggesting normal granulosa cell differentiation.

Similar to females, *S100a4-Cre;Ptch1*$^{fl/fl}$ homozygous mutant males also exhibit hypogonadism (Figure 2 and Table 2). At 8 weeks of age, the size and weight of testis, epididymis and seminal vesicles in mutant mice were reduced compared to those of wild-type control mice (Figure 2A and Table 2). Because the body weight of mutant mice was also significantly reduced at this age compared to controls, the weights of male reproductive tissues were normalized to body weight. After normalization, testicular and epididymal weights of homozygous mutants were not significantly different from controls, whereas seminal vesicles remained hypomorphic. In addition, sperm count was drastically reduced and sperm motility was severely impaired (Table 2). These defects suggest reduced testosterone production. Indeed, serum testosterone levels tend to be lower in the mutants compared to controls (Figure 2B), and genes crucial for testosterone production including *Cyp11a1*, *Cyp17a1* and *Lhcgr* exhibited significantly reduced testicular mRNA levels (Figure 2C). In contrast, mRNA expression of *Fshr* and *Amh* was similar in mutant and control mice, suggesting normal development and function of Sertoli cells. To explore the basis of the abnormal spermatogenesis phenotype, periodic acid-Schiff (PAS) staining was applied to testis tissue sections (Figure 2D). While many seminiferous tubules appeared normal in the mutants, with germ cells present at all developmental stages, sporadic abnormal seminiferous tubule structures (impaired spatial hierarchy of spermatogenesis, areas of vacuoles, and multinucleated spermatids) were also observed. Together, these data document hypogonadism in both adult female and male homozygous *S100a4-Cre;Ptch1*$^{fl/fl}$ mutant mice.

Hypogonadism in Ptch1 mutant mice develops during the transition from puberty to adult. To determine when hypogonadism arises in *Ptch1* mutant mice, we assessed their reproductive tissues at 4 (females) and 5 (males) weeks of age. At this age, no differences in body or reproductive organ weights were observed in either males or females between controls and mutants (Table 1 and 2). Ovaries from *Ptch1* mutants were histologically comparable to their wild-type littermates, with the presence of CL and follicles at all developmental stages (Figure 3A).

These observations are consistent with normal serum FSH and LH levels in the mutant mice at this age (Supplemental Figure 1A). Moreover, 5 week old, wild-type, heterozygous and homozygous *Ptch1* mutant females ovulated similar numbers of oocytes upon super-ovulation (Figure 3B). When the same superovulation regimen was administered to mice at 8 weeks of age, histological assessment revealed that by 20 hour (h) post-human chorionic gonadotropin (hCG), multiple early CL had formed in wild-type females, but ovulation and luteinization failed to occur in the majority of pre-ovulatory follicles in the mutants, where oocytes and their surrounding cumulus cells were trapped in large antral follicles (Figure 3C). Consistent with these observations, significantly fewer oocytes were found in the oviduct of homozygous *Ptch1* mutant females at 20 h post-hCG (Figure 3D). Despite the lack of ovulation and failure of luteinization in these mutant mice, exogenous gonadotropin did rescue follicle development from pre-antral to pre-ovulatory stages. Taken together, these data indicate that the development of reproductive tissues and the onset of puberty in *S100a4-Cre;Ptch1$^{fl/fl}$* mutant females and males are normal, and that hypogonadism develops during the transition between puberty and adulthood.

S100a4-Cre is expressed in CD45$^+$ hematopoietic cells in the gonads. We employed *S100a4-Cre;Ptch1$^{fl/fl}$* mutants that also expressed Cre-driven green fluorescent protein (GFP) (*S100a4-Cre;Ptch1$^{fl/fl}$;mTmG)* to determine what cell types in the gonads express *S100a4-Cre*. In these mice, *R26^{mTmG}* drives expression of a membrane-associated red fluorescent protein that is switched to membrane-associated GFP upon Cre-mediated recombination, allowing *in vivo* lineage tracing of all cells in which recombination has occurred (GFP$^+$ cells). Immunofluorescent (IF) staining in ovaries of reporter-positive controls at 8 weeks of age demonstrated GFP$^+$ cells throughout the surrounding stromal tissue of growing follicles, dispersed in the CL, and in clusters at sites of degenerating follicles (Figure 4A, upper left). Granulosa cells or oocytes of growing follicles were negative for GFP. GFP$^+$ cells in the *S100a4-Cre;Ptch1$^{fl/fl}$;mTmG* mutant mice exhibited a similar pattern of distribution except that there were no CL (Figure 4A, upper right).

Surprisingly, co-IF staining of GFP and S100A4 revealed very few co-stained cells (Figure 4A, lower panels). This staining also revealed very few S100A4-positive cells in the stromal-interstitial tissue of the ovary, which appeared to be true during earlier development (days 4, 12 and 22, Supplemental Figure 1B).

Because S100A4 is more commonly known as fibroblast-specific protein 1 (FSP1), and widely used as a marker for fibroblast cells, we performed co-IF of GFP with fibroblast markers vimentin and ACTA2 to determine whether these cells are expressing Cre-dependent GFP. Because neither vimentin nor ACTA2 co-localized with GFP in the ovaries of control reporter-positive mice (Figure 4B), the GFP^+ cells do not appear to be fibroblasts; based on their morphology and distribution, they appeared instead to be infiltrating immune cells. This is supported by the observation that there were far fewer GFP^+ cells in the ovaries of immature mice (day 22, Supplemental Figure 1B) compared to adults, suggesting these cells are recruited by gonadotropins in a cycling female, similar to intra-ovarian immune cells (24-26). To test whether GFP^+ cells express immune cell markers, we performed immuno-staining for GFP and CD45, a marker for cells of hematopoietic origin, on adjacent sections of the ovary from *S100a4-Cre;mTmG* reporter mice. GFP and CD45 positive cells exhibited a similar pattern of distribution, suggesting they are the same population of cells (Figure 4C). This observation was further confirmed by flow cytometry analyses of dispersed GFP^+ cells from ovaries of *S100a4-Cre;mTmG* reporter control mice, in which about 90% of GFP^+ cells also expressed CD45 (Figure 4D). It is likely that deletion of *Ptch1* by *S100a4-Cre* occurred during early stage specification of $CD45^+$ hematopoietic cells, as both S100A4 and PTCH1 are expressed in hematopoietic cells in human bone marrow (Supplemental Figure 1C), and *S100a4*-Cre is expressed as early as embryonic day 8.5 (27).

We also examined the morphology and distribution of GFP^+ cells in the testis. Immunohistochemistry (IHC) staining demonstrated that GFP^+ cells were within the stromal-interstitial tissue of the testis (Figure 4E, lower left). In contrast to the ovary, $S100A4^+$ cells were

prevalent in the testis. They were located in interstitial space (Figure 4E, upper right), and most co-localized with GFP$^+$ cells (Figure 4E, lower right). The stromal-interstitial localization of GFP$^+$ and S100A4$^+$ cells resembled that of PTCH1 itself, as revealed by Xgal staining in the testis of *Ptch1*-Xgal mice (Figure4E, upper left). Based on the localization of GFP$^+$ cells, we further assessed whether *S100a4-Cre* is expressed in Leydig cells. This appeared not to be the case as indicated by the lack of co-localization of GFP and CYP17A1, a marker for steroidogenic Leydig cells (Figure 4F). Instead, the GFP$^+$ cells intermingle with but were distinct from CYP17A1$^+$ cells, suggesting they may be macrophages (28). Together, these data indicate that *S100a4-Cre* positive cells within the stromal-interstitial tissue of the gonads and are mostly CD45$^+$ hematopoietic cells.

Gonad-extrinsic factors contribute to hypogonadism in Ptch1 mutant mice. In the gonads of adult mice, although *S100a4-Cre* is mostly active in cells of hematopoietic lineages, this does not exclude the possibility that *S100a4-Cre* is expressed in other cell types during early gonadal development, leading to hypogonadism through gonad-intrinsic mechanisms. To test whether this might be the case, ovaries were transplanted from 4 week old *S100a4-Cre;Ptch1$^{fl/fl}$;mTmG* mutant mice to their control littermates (*Ptch1$^{fl/fl}$;mTmG*). Ovaries were also transplanted between control mice for comparison. At 8 weeks of age, ovarian function was rescued in ovaries transplanted from mutant to control mice (Figure 5A), in contrast to un-transplanted ovaries of mutant mice, in which follicles rarely grow to acquire an antral cavity (Figure 1B). Ovaries transplanted from mutant to control mice had antral follicles (F) and multiple CL, similar to those of transplanted ovaries from control mice (Figure 5B). Notably, despite the presence of CD45$^+$ cells in ovaries transplanted from mutant mice, there were no GFP$^+$ cells four weeks after the transplantation (Figure 5C), suggesting that *S100a4-Cre*-expressing cells in the ovary are mostly non-resident hematopoietic cells. We also attempted to test whether grafting wild-type bone marrow cells rescues fertility and pituitary endocrine functions in the *S100a4-Cre;Ptch1$^{fl/fl}$* mutant mice.

Unfortunately, we were not able to collect interpretable data because, even at a reduced dose, the irradiation used to first deplete host bone marrow hematopoietic cells also depleted most of the oocytes. Taken together, these results indicate that hypogonadism in female mutants is caused primarily by gonad-extrinsic factors.

The most important gonad-extrinsic factors regulating fertility are FSH and LH produced by the pituitary gland. Therefore, we measured serum FSH and LH in *S100a4-Cre;Ptch1*$^{fl/fl}$ mutants. At 8 weeks of age, serum concentrations of FSH and LH were both reduced in male mutants compared to wild-type control littermates (Figure 5D, upper panels). Because female *Ptch1* mutants do not cycle (22), we measured serum FSH and LH in mutants and random cycling control littermate females, which displayed large variability (Figure 5D, lower panel). While serum FSH tended to be lower in the female mutants, the difference from controls was not significant. In contrast, serum concentrations of LH were significantly lower in the mutant females relative to controls.

To investigate whether reduced gonadotropin production in *S100a4-Cre;Ptch1*$^{fl/fl}$ mutant mice was caused by disrupted feedback signals from the gonads, mutant female mice were ovariectomized at 4 weeks of age and mRNA levels for (luteinizing hormone beta) *Lhb* and follicle stimulating hormone beta (*Fshb*) in the pituitary were measured by qPCR at 8 weeks of age. Consistent with serum concentrations of FSH and LH, *Lhb* mRNA was reduced and *Fshb* was normal in the intact mutant females (Figure 5E). Following ovariectomy, levels of *Lhb* and *Fshb* mRNA increased in the control mice; in the mutants, no increase occurred for *Fshb* mRNA, whereas *Lhb* mRNA increased but remained significantly lower compared to controls. The relative mRNA levels of *Fshb* and *Lhb* were consistent with significantly reduced serum FSH and LH levels after ovariectomy in *Ptch1* mutants compared to controls (Supplemental Figure 1D). These results indicate that pituitary gonadotropin production is impaired in both male and female *S100a4-Cre;Ptch1*$^{fl/fl}$ mutant mice, likely contributing to their hypogonadism.

Adult Ptch1 mutant mice exhibit severe and sexually dimorphic abnormalities in pituitary endocrine functions. To understand the cause of impaired gonadotropin production in *S100a4-Cre;Ptch1$^{fl/fl}$* mutant mice, we measured mRNA levels of key genes regulating pituitary endocrine functions and found alterations in multiple pathways in these mutants at 8 weeks of age (Figure 6A). Specifically, mRNA levels of the gene encoding the alpha subunit of glycoprotein hormones (*Cga*) were drastically reduced in both sexes. The alpha subunit of glycoprotein hormones is required for the biosynthesis of LH, FSH and TSH. In *S100a4-Cre;Ptch1$^{fl/fl}$* mutant mice, thyroid stimulating hormone subunit beta (*Tshb*) mRNA levels were elevated in both sexes, consistent with previous studies where *Tshb* mRNA levels were elevated in *Cga* knockout mice (29). Also consistent with data from the ovariectomy experiment described above, the levels of mRNA for *Fshb* was normal in the mutant females, whereas *Lhb* in the mutant females, as well as *Lhb* and *Fshb* in the mutant males, all had reduced mRNA levels. These abnormalities are unlikely related to defective differentiation or proliferation of gonadotropes as evidenced by normal levels of mRNA for gonadotropin releasing hormone receptor (*Gnrhr*) (Supplemental Figure 2B). Similarly, given the normal levels of mRNA for POU domain, class 1, transcription factor 1 (*Pou1f1*) (Supplemental Figure 2B), differentiation of thyrotropes, somatotropes, and lactotropes are likely unaffected by *Ptch1* ablation. While growth hormone (*Gh*) mRNA levels were elevated in both sexes, mRNA levels of prolactin (*Prl*) and *pro-opiomelanocortin-alpha* (*Pomc*, encodes precursor of ACTH) were elevated in female but not male mutants. Despite the increased transcript levels of *Pomc* in female mutants, serum corticosterone levels were normal in both males and female mutants (Supplemental Figure 2C). In contrast to 8 weeks of age, transcript levels for all the above mentioned genes were normal at 4 weeks of age in female mutants and 5 weeks of age in male mutants (the age of puberty onset in each sex, respectively) (Figure 6B), except for a decrease in mRNA levels of *Cga* in male mutants at 5 weeks of age. The mostly normal transcript levels in the mutant mice at 4~5 weeks of age are consistent with their normal pituitary morphological appearances at 4.5 weeks of age (Supplemental Figure 2A). With the severely abnormal pituitary

endocrine function, it is not surprising that *S100a4-Cre;Ptch1*$^{fl/fl}$ mutant mice frequently die at around 12 weeks of age. Together, these data indicate that abnormal pituitary endocrine function in *S100a4-Cre;Ptch1*$^{fl/fl}$ mutant mice occurs during the transition between the onset of puberty and adulthood.

Given the above described range of abnormal gene expression in the pituitaries of *S100a4-Cre;Ptch1*$^{fl/fl}$ mutant mice at 8 weeks of age, it was not surprising that the pituitary gland in these mutants also exhibited morphological abnormalities. Pituitary glands from both sexes are consistently smaller in the mutants, with frequent reddish appearance, suggesting that they may be hemorrhagic (Figure 6C). We employed transmission electron microscopy (TEM) to further understand how different endocrine cell types in the pituitary were affected in these mutant mice (Figure 6D). While gonadotropes appeared normal in the mutants of both sexes, thyrotropes in both male and female mutants displayed extensive expansion of dilated endoplasmic reticulum (ER), which was also observed in *Cga* knockout mice and suggests ER stress (29). Secretory granules in thyrotropes distributed evenly across the cytoplasm in the control mice, but clustered near the cytoplasmic membrane in the mutant mice, suggesting abnormal production of TSH. Somatotropes exhibited abnormal morphology in female mutants, in which they had a shrunken appearance, with irregular cytoplasmic membrane and smaller size. These results demonstrate that *S100a4-Cre;Ptch1*$^{fl/fl}$ mutant mice have severe and sex-specific abnormalities in pituitary endocrine functions that are not restricted to gonadotropes.

To determine whether *S100a4-Cre* activity disrupts HH signaling activity in the adult pituitary gland, we analyzed expression of transcripts for key pathway components at 8 weeks of age in both male and female mice (Figure 6E). Levels of mRNA for *Ptch1*, *Ptch2* and *Gli2* were increased in the female mutants, and levels of *Dhh*, *Ptch1*, *Gli1* and hedgehog-interacting protein (*Hhip*) were increased in the male mutants as compared to controls. These results indicate that HH signaling is active in the adult pituitary and increased due to *S100a4-Cre* activity. In particular, the increase in the levels of *Ptch1* mRNA must originate from cells that do not express *S100a4-*

317 *Cre*, suggesting paracrine crosstalk between Cre-expressing cells and other cell types in the
318 anterior pituitary. To test this hypothesis, we aimed to localize *Ptch1* mRNA in the adult anterior
319 pituitary using RNA *in situ* hybridization (Supplemental Figure 4A). Although the signal for *Ptch1*
320 mRNA was too low to conclude its specific cellular localization, it tended to be stronger in the
321 mutants of both sexes compared to controls, consistent with qPCR results.

322 Adiposity and adipose tissue-derived factors, such as leptin, are known to play a role in
323 regulating pituitary endocrine function (30). We observed that *S100a4-Cre;Ptch1*$^{fl/fl}$ mutant mice
324 have severely reduced adiposity by 8 weeks of age (Supplemental Figure 2E), and suspected
325 that this might be a major cause of the abnormal pituitary function. To test this, we analyzed
326 pituitaries from mice with ablation of the gene Berardinelli-Seip congenital lipodystrophy 2 (*Bscl2*,
327 also known as seipin) (31, 32). *Bscl2* knockout mice have similar reductions in adiposity as
328 *S100a4-Cre;Ptch1*$^{fl/fl}$ mutant mice, but normal levels of mRNA for key pituitary functional genes
329 (Supplemental Figure 2F), indicating that the reduced adiposity in *S100a4-Cre;Ptch1*$^{fl/fl}$ mutant
330 mice is not sufficient to explain their abnormal pituitary function. We also measured the transcript
331 levels of hypothalamic genes that are critical for pituitary function (Supplemental Figure 3).
332 Notably, transcript levels of KiSS-1 metastasis-suppressor (*Kiss1*) and growth hormone releasing
333 hormone (*Ghrh*) were significantly reduced in the hypothalamus of both male and female *S100a4-*
334 *Cre;Ptch1*$^{fl/fl}$ mutant mice. There was no difference in transcript levels of gonadotropin releasing
335 hormone 1 (*Gnrh1*), thyrotropin releasing hormone (*Trh*), corticotropin releasing hormone (*Crh*),
336 or somatostatin (*Sst*). These data suggest that hypothalamic factors contribute to but cannot fully
337 account for the pituitary phenotype in *S100a4-Cre;Ptch1*$^{fl/fl}$ mutant mice. We also measured
338 transcript levels of *Ptch1* in hypothalamus of control and mutant mice but did not detect any
339 difference (Supplemental Figure 3), indicating that altered hypothalamus gene expression in the
340 mutants is caused not by *Ptch1* ablation in the hypothalamus, but rather by feedback from
341 peripheral tissues.

342

Deletion of Ptch1 by S100a4-Cre in CD45⁺ hematopoietic cells of the anterior pituitary, in particular folliculo-stellate (FS) cells, alters pituitary local microenvironment. To understand the underlying cause of the severe pituitary abnormalities in *S100a4-Cre;Ptch1$^{fl/fl}$* mutant mice, we first determined the pituitary cell type in which *S100a4-Cre* is expressed by IF staining of *Cre*-dependent expression of GFP (Figure 7A). In the anterior pituitary, GFP⁺ cells were dispersed throughout the tissue (Figure 7A, upper panel). The cytoplasmic membrane localized GFP revealed multiple cellular protrusions (Figure 7A, lower panels). The distribution and morphology of GFP⁺ cells resembled those described previously for FS cells, which are pituitary-specific non-endocrine cells that can influence endocrine cell function through secreted molecules and direct contact-dependent intercellular interactions (33-35). S100 proteins, in particular S100β, are expressed by FS cells in the anterior pituitary in rats but not mice (35). We postulated that perhaps instead of S100β, FS cells in the adult mouse pituitary express S100A4. This appears not to be the case as IF staining revealed very few cells expressing S100A4 protein (Supplemental Figure 4C, left), suggesting that similar to the ovary, *S100a4*-expressing cells in the adult pituitary are not resident but infiltrate from circulation. To determine whether GFP⁺ cells are indeed FS cells, we performed immunogold labeling of GFP on ultra-structural sections of pituitary tissue followed by TEM. In both male and female *S100a4-Cre;mTmG* reporter-positive control mice that express GFP, numerous anti-GFP immunogold particles were identified in FS cells based on their ultrastructural features (Figure 7B, upper panels, arrows); in contrast, only minimal immunogold signals were observed in other cells such as endothelial cells (EC) (Figure 7B, lower left). *Ptch1$^{fl/fl}$* mice that do not express GFP were used as additional controls and only minimal immunogold signals were present in FS cells of these mice (Figure 7B, lower panels, arrows). We further demonstrated that a small subpopulation of *S100a4-Cre*-expressing cells also uptake β-Ala-Lys-Nε-AMCA (Supplemental Figure 4B), which is taken up specifically by the FS cells of the anterior pituitary in rat and fish (36, 37). Similar to our observations in the ovary (Figure 4), approximately 90% of GFP⁺ cells also expressed CD45 (Figure 7C). The hematopoietic cell identity of GFP⁺ cells

was further supported by co-IF staining of *S100a4-Cre*;tdTomato with that of F4/80 (marker for monocytes such as macrophages) (Supplemental Figure 4C, right) (38). Taken together, these results indicate that *S100a4-Cre* activity in the anterior pituitary gland was restricted to $CD45^+$ cells derived from the hematopoietic lineage, such as FS cells and possibly also macrophages.

Altered FS cell function contributes to pituitary abnormalities of Ptch1 mutant mice through sexually dimorphic mechanisms. We therefore assessed whether *S100a4-Cre* activity in FS cells of *S100a4-Cre;Ptch1$^{fl/fl}$* mutant mice might explain their severely impaired pituitary endocrine function. At the ultra-structural level, TEM revealed that while many FS cells in the mutants had normal appearance, there were also many FS cells with shrunken cytoplasm, shortened cellular protrusions, and nuclear fragmentation that are typical of apoptotic cells (Figure 7D). Cellular protrusions in FS cells are important for their network formation and interactions with endocrine cells in the pituitary (36, 37, 39, 40), hence abnormalities in these protrusions likely contribute to the endocrine phenotype in the *S100a4-Cre;Ptch1$^{fl/fl}$* mutant mice.

To assess the contribution of FS cells to the pituitary abnormalities in these mutants, we measured mRNA levels for genes that are associated with pituitary local microenvironment and expressed prominently in FS cells (Figure 7E) (39), including follistatin (*Fst*), interleukin 6 (*Il6*), vascular endothelial growth factor A (*Vegfa*), nitric oxide synthase 1 (*Nos1*), fibronectin 1 (*Fn1*) and macrophage migration inhibitory factor (*Mif*). Among these, only *Vegfa* showed no difference between mutants and controls. *Fst* was increased in the mutants of both sexes; the other genes exhibited sexually-dimorphic alterations in mutants compared to controls, with increased transcripts of *Il6* and *Nos1* in females and *Fn1* in males. Transcript levels of *Mif* were decreased in female but not male mutants. Except for *Ihh*, none of these genes nor key genes within the HH signaling pathway showed abnormal levels of mRNA in the *Bscl2* knockout mice (Supplemental Figure 4, D and E), indicating their abnormal expression in the *S100a4-Cre;Ptch1$^{fl/fl}$* mutant mice was not simply due to reduced adiposity. These results indicate that the functional disruption of

pituitary CD45^{+} cells, including FS cells, contributes to the endocrine abnormalities in *S100a4-Cre;Ptch1$^{fl/fl}$* mutant mice.

Discussion

Results in this report highlight a new function of CD45$^+$ hematopoietic cell lineages in regulating fertility and pituitary endocrine functions. Using the *S100a4-Cre;Ptch1*$^{fl/fl}$ transgenic mouse model and lineage tracing with the *mTmG* reporter in the ovary, testis and pituitary, we have demonstrated that cells with *S100a4-Cre*-dependent GFP expression are present in each tissue and are mostly CD45 positive. GFP$^+$CD45$^+$ cells are associated primarily with theca/stroma cells and atretic follicles in ovaries and Leydig cells in the testis. Moreover, in the pituitary we show that the GFP$^+$ cells are likely a heterogeneous population with FS cells as a subset. Our studies provide novel *in vivo* evidence that disruption of *Ptch1* signaling in CD45$^+$ hematopoietic cells, including FS cells, has functional impact on multiple pituitary endocrine cells. Most notable is the decreased expression of *Cga* and gonadotropin production. Thus, *S100a4-Cre;Ptch1*$^{fl/fl}$ mutant mice provide a novel model by which to understand how HH signaling in hematopoietic cells impacts adult-onset hypogonadotropic hypogonadism and pituitary endocrine disorders.

The S100a4-Cre mouse line is a useful tool to study in vivo functions of hematopoietic cells in endocrine organs. Results reported here demonstrate that in reproductive organs including the ovary, testis and pituitary, the majority of cells expressing *S100a4-Cre* are CD45$^+$ cells of hematopoietic lineages (Figures 4 and 7; Supplemental Figure 1). Furthermore, we observe tissue-specific cell type localization of S100A4 and *S100a4-Cre* (as indicated by the GFP reporter expression), in the testis versus the ovary. In the testis, immuno-labeling of S100A4 and GFP appear to be in the same populations in the interstitial cells surrounding the seminiferous tubules that are not CYP17A1$^+$ Leydig cells (Figure 4E). In the ovary, GFP$^+$ cells are widespread in stromal tissue and apoptotic follicles but immuno-staining reveals very few S100A4-expressing cells in the stroma-interstitial tissues, and even fewer cells express both GFP and S100A4 (Figure 4A). These observations suggest that while GFP$^+$ cells in the testis are resident, the GFP$^+$ cells present in the ovary are derived from circulation. This conclusion is further supported by the ovarian

transplant experiment (Figure 5C) in which GFP$^+$ cells were absent in ovaries of *S100a4-Cre;Ptch1$^{fl/fl}$;mTmG* mutant mice that were transplanted to wild-type (GFP$^-$) hosts. Infiltrating immune cells in the ovary are involved in apoptosis, ovulation and luteinization (24, 41). Because the *S100a4-Cre;Ptch1$^{fl/fl}$* mice are infertile, fail to ovulate and exhibit a reduced response to superovulation at 8 weeks of age (Figures 3C and 3D), it is likely that the *Ptch1* deficient immune cells present in the ovary have reduced ability to control key events mediating ovulation and luteinization. Alternatively, failure of ovulation in these mice with exogenous gonadotropins administration may also be a consequence of long-term low LH levels.

In the anterior pituitary, *S100a4-Cre* appears to be active predominantly in hematopoietic cells, including FS cells. Similar to our observations in the ovary, we detected very few cells with expression of S100A4 protein in the anterior pituitary, suggesting the GFP$^+$ cells are hematopoietic cells infiltrating from the circulation. Future studies are needed to test whether this is indeed the case. Specifically, a detailed analysis of S100A4 and *S100a4-Cre;mTmG* expression from embryonic development to neonatal, juvenile and adulthood should help clarify the origin and dynamics of pituitary hematopoietic/immune cells. Although *S100a4-Cre* activity is restricted to CD45$^+$ cells in the anterior pituitary, we cannot entirely rule out that the pituitary phenotype in *S100a4-Cre;Ptch1$^{fl/fl}$* mutants is related to, or caused by, *S100a4-Cre* activity in non-pituitary tissues. For example, in addition to *S100a4-Cre* activity in the gonads, S100A4 protein has been reported to be expressed in astrocytes of the brain (42). GFP expression driven by S100β promoter in rat is also detected in bones and adipose tissues (43). However, we have demonstrated that pituitary gonadotropin deficiency in *S100a4-Cre;Ptch1$^{fl/fl}$* mutants is not dependent on gonadal factors (Figure 5E); in addition, a transgenic mouse line that is depleted of adipose tissues (*Bscl2$^{-/-}$* mice) does not exhibit a similar pituitary phenotype as in the *S100a4-Cre;Ptch1$^{fl/fl}$* mutants, supporting that reduced adiposity in the latter is not the primary cause of their pituitary abnormalities. Instead, our current data suggest that pituitary endocrine disorders can arise via local interactions. Specifically, in the *S100a4-Cre;Ptch1$^{fl/fl}$* mutant mice we observed

FS cells with morphological alterations typical of apoptotic cells (Figure 7D). We also detected abnormal mRNA levels of transcripts that are enriched in FS cells and encode important factors within the pituitary local microenvironment, such as *Fst*, *Fn1* and *Il6* (Figure 7E). Although it is possible that these alterations in FS cells are a consequence, instead of a cause, of pituitary dysfunction due to pituitary-extrinsic factors, these data suggest that FS cells contribute to pituitary phenotype observed in *S100a4-Cre;Ptch1*$^{fl/fl}$ mutant mice. Notably, FS cells are a heterogeneous population and future studies are needed to clarify their classification as and functional relationship with hematopoietic/immune cells.

While our current findings focus on the gonads and the pituitary, there are also effects of *Ptch1* ablation by *S100a4-Cre* on other organs, such as previously reported in the mammary gland (22). These phenotypes together lead to a key outstanding question: to what extent do the phenotypes observed in individual organs derive from local/resident versus circulating hematopoietic cells? What are the compounding effects of pituitary hormone disorders on these phenotypes? The answer to these questions require substantial advances with regard to the relationship between local/resident and circulating hematopoietic cells in terms of their differentiation and function in individual tissue types.

Cells of hematopoietic lineages as potential targets of HH signaling in the tissue microenvironment. HH signaling regulates numerous developmental processes mainly as a mediator of crosstalk between parenchymal and mesenchymal tissue compartments (16). Although HH signaling network members are expressed in T and B cells and modulate the specification and development of these cells (44-46), functions of HH signaling in non-B or T cells remain to be characterized. In the testis, for example, while HH ligands are expressed in Sertoli cells, the signaling receptor *Ptch1* is expressed in the stromal-interstitial tissues surrounding the seminiferous tubules and regulates Leydig cell differentiation and function (6). Our data suggest that at least in the adult testis, the HH signaling receptor PTCH1 is likely expressed in CD45^{+} cells

of hematopoietic lineages. Thus it is tempting to speculate that these cells may also be targets of HH ligands from Sertoli cells (or other cells), and perhaps, by providing local production of cytokines, can impact steroidogenesis of adjacent Leydig cells. In human anterior pituitary, PTCH1 is expressed at detectable levels and its localization correlates with that of FS cells (47). In addition, the adult human pituitary is responsive to manipulations of canonical HH signaling activity (48). In the *S100a4-Cre;Ptch1*$^{fl/fl}$ mutant mice, transcript levels of *Ptch1* are increased in the pituitaries of both sexes (Figure 6E). This counterintuitive finding supports that hedgehog signaling can be activated in the adult mouse pituitary, and suggests that the increased transcript level of *Ptch1* derives from non-*S100a4* cell lineages in the pituitary, reflecting paracrine interactions and alterations. Human genome-wide association study (GWAS) data shows that mutations in HH signaling components, including *GLI2* and *PTCH1*, are involved in pituitary hormone disorders and adenomas (8, 49, 50). Therefore, future studies aimed to elucidate whether HH signaling regulates the differentiation and/or function of hematopoietic cells in adult ovary and pituitary may provide novel insights into the physiology and dysfunction of these two organs.

Insights into the function, expression, and regulation of Cga. Regarding pituitary endocrine function, the most profound and consistent phenotype in the *S100a4-Cre;Ptch1*$^{fl/fl}$ mutant mice in the reduced expression of *Cga* mRNA in both sexes (Figure 6A). Reduced *Cga* transcript levels are also the earliest change we detected in the pituitaries of these mice, occurring at 5 weeks in the mutant males, when no other physiological abnormality was detected. Low *Cga* expression and the associated reduction in FSH and LH levels exert a major impact on the gonadal phenotypes we observe in the *S100a4-Cre;Ptch1*$^{fl/fl}$ mutants. These mutant mice share similarities with the *Cga* knockout mice (*Cga*$^{-/-}$) that exhibit profound hypogonadism during post-neonatal development when the gonads become gonadotropin-dependent (51). Despite the severe hypogonadotropic phenotype, the size and number of pituitary gonadotropes appeared normal

and comparable in both male and female mutants (51). In addition, thyrotropes in both mutants exhibited dilated ER, likely reflecting the lack of negative feedback due to diminished *Cga* expression and thyroid hormone production. By early adulthood a significant reduction in body weight was observed in both sexes, likely associated with thyroid hormone dysregulation, with the onset of reduction occurring earlier in *Cga*$^{-/-}$ mice (3 weeks of age) compared to *S100a4-Cre;Ptch1*$^{fl/fl}$ mutant mice (after 5 weeks of age). It is possible that because the sizes of pituitaries from *S100a4-Cre;Ptch1*$^{fl/fl}$ mutant mice were significantly smaller compared to controls at 8 weeks of age, the alterations in pituitary gene expression may either reflect reduced numbers of a specific endocrine cell population, or alternatively, reduced transcript levels in individual endocrine cells.

Despite many similar phenotypic features between *Cga*$^{-/-}$ and *S100a4-Cre;Ptch1*$^{fl/fl}$ mutant mice, differences are also present: transcript levels of *Gh* and *Prl* are reduced in *Cga*$^{-/-}$ mutants but increased in *S100a4-Cre;Ptch1*$^{fl/fl}$ mutant (Figure 6A); the number of lactotropes is significantly reduced in *Cga*$^{-/-}$ mutants while *Prl* transcript level is significantly increased in female *S100a4-Cre;Ptch1*$^{fl/fl}$ mutant mice. These differences suggest additional mechanisms, independent from *Cga,* through which *Ptch1* deletion may lead to pituitary abnormalities or, alternatively, a developmental stage-specific effect of *Cga* deficiency. It is unclear how some endocrine cells appear to have enhanced while others have diminished hormone encoding gene expression in the *S100a4-Cre;Ptch1*$^{fl/fl}$ mutant mice. However, this is plausible given a previous proposed role of pituitary immune cells, in particular FS cells, in forming an intra-pituitary network and coordinating activities of different endocrine cell types (36). Furthermore, even though we did not find any report on human patients with concurrence of low TSH and high GH, such divergent changes in distinct pituitary endocrine axes are also observed in other transgenic mouse models, such as in mice with *Foxp3* and *Zbtb20* ablation, respectively (52, 53). Taken together, our findings raise the possibility that pituitary hematopoietic/immune cells play a role in regulating *Cga* expression via their interactions with endocrine cells, presumably involving HH signaling.

CD45⁺ hematopoietic cells contribute to pituitary sexual maturation and local microenvironment. During the transition from puberty to adulthood, the pituitary gland undergoes drastic structural and functional re-organization. For example, numbers of gonadotropes and somatotropes increase and the vascular network of the gland elaborates substantially (15). Sexually dimorphic features are also prominent: a transient increase in the clustering of somatotropes during puberty is observed only in males but not females (54, 55). Although signals from the hypothalamus are key drivers of these changes during pituitary sexual maturation, the extent to which pituitary-intrinsic regulatory mechanisms contribute to these processes remains to be defined (15, 56). Our current data provide evidence for a previously underappreciated role of a CD45⁺ cell population including FS cells, in regulating pituitary sexual maturation. We find that pituitaries of both male and female *S100a4-Cre;Ptch1$^{fl/fl}$* mutants display normal expression of key endocrine genes at the onset of puberty, but severe functional defects by early adulthood (Figure 6A and 6B). Compared to congenital hypogonadotropic hypogonadism, which is extremely rare and mostly caused by mutations in gonadotropin releasing hormone (GnRH) signaling pathway (57), acquired adult-onset hypogonadotropic hypogonadism is both much more common and less well understood (58). Our current findings suggest a role for pituitary hematopoietic/immune cells in the etiology of acquired hypogonadotropic hypogonadism.

We also identified sexually dimorphic expression alterations of several FS cell-enriched local growth factors, cytokines, and extracellular matrix components in *S100a4-Cre;Ptch1$^{fl/fl}$* mutants. While the mechanisms by which these factors may contribute to the pituitary phenotype remains to be determined, previous studies show that their production does not occur until the time around puberty, supporting their role in this critical transition period (59). While the mechanism of how hematopoietic cells, including FS cells, regulate pituitary endocrine cell functions remains incompletely understood, at least two potential mechanisms may be at work: 1) pituitary hematopoietic cells exert distinct effects on different pituitary endocrine cell types; and/or 2) they exert effects (such as on extracellular matrix structure and tissue organization) that can

impact different pituitary endocrine cells in distinct ways. Another possibility is that ablation of *Ptch1* in *S100a4* cell lineages alters the recruitment and/or activation of other immune cells, such as regulatory T cells. This hypothesis is based on the resemblance of multiple phenotypes between *S100a4-Cre;Ptch1*$^{fl/fl}$ mice and the “scurfy mice”, in which the regulatory T cell transcription factor *Foxp3* is deleted (53, 60-62). Similar to the *S100a4-Cre;Ptch1*$^{fl/fl}$ mutant mice, *Foxp3* mutant mice are also infertile, and exhibit aberrant transcript levels of several key pituitary endocrine genes. Future studies are needed to test these hypotheses and define the mechanism by which immune cells regulate pituitary endocrine functions.

In summary, the *S100a4-Cre;Ptch1*$^{fl/fl}$ mouse model provides strong evidence that PTCH1-dependent HH signaling activity in CD45^{+} cells plays a role in adult-onset hypogonadotropic hypogonadism. Our findings also corroborate the conclusion from previous studies that systemic defects caused by *Ptch1* deletion in these mice are responsible for the stunted mammary duct development (22, 23). Disruption of HH signaling in pituitary hematopoietic cells may be a previously underappreciated cause of hypogonadotropic hypogonadism and other pituitary hormone disorders.

Methods

Real-time Q-PCR analysis of gene expression, histology and immunostaining, ovariectomy and ovarian transplant, and flow cytometry are detailed in Supplemental Methods.

Animal Models and treatments. Dr. Brandon Wainwright kindly provided mice with the *Ptch1*^{c} allele (*Ptch1*^{fl} here) (63). Animals carrying the *S100a4* promoter-driven *Cre* recombinase were a gift from Dr. Eric Neilson (Vanderbilt University, Nashville, TN, USA). In this model, Cre recombinase is expressed in fibroblasts and some myeloid cells (27). We also used mice carrying *mTmG* (Jackson Laboratory, Gt(ROSA)26Sor$^{tm4(ACTB-tdTomato,-EGFP)}$Luo/J) and tdTomato (Jackson Laboratory, Gt(ROSA)26Sor$^{tm14(CAG-tdTomato)}$Hze) *Cre* reporter. Breeding was accomplished by crossing *S100a4-Cre;Ptch1*$^{fl/+}$ males with *Ptch1*$^{fl/+}$or *Ptch1*$^{fl/fl}$ females of different genotypes for *Ptch1*. Dr. Martin J. Cohn (University of Florida, Gainesville, FL, USA) kindly provided the testis of *Ptch1*-LacZ mice (64).

For superovulation studies, animals at post-natal day 22 or 8 weeks of age were injected with 5 IU equine chorionic gonadotropin (eCG) followed by 5 IU hCG 48 hours later, with harvest 16 hours after hCG treatment Sigma Aldrich, CG5-1VL). To measure the concentration of hormones in the circulation, male mice were caged individually in the absence of female for a week prior to serum collection. Serum hormone levels were assay by the University of Virginia Ligand Core (N≥6 samples per genotype).

Ovariectomy and ovarian transplant. To determine whether gonadal factors are contributing to pituitary phenotypes in the *S100a4-Cre;Ptch1*$^{fl/fl}$ mutant mice, we surgically removed both of their ovaries at 4 weeks of age. Ovaries were also removed from their wild-type littermates at the same age for comparison. Pituitary function were examined at 8 weeks of age after ovariectomy. To determine whether the hypotrophic ovaries in *S100a4-Cre;Ptch1*$^{fl/fl}$ mutant mice were caused by ovarian intrinsic versus extrinsic factors, ovaries of these mutant mice were transplanted into the

bursa of wild-type littermates at 4 weeks of age. At the same age, ovaries were also transplanted from wild-type mice to their wild-type littermates as controls. Ovarian tissues were collected and analyzed at 8 weeks of age, 4 weeks after the transplantation, to assess their function and health. Four mutant and four control mice were used for each experiment.

Sperm count and sperm motility assessment. The cauda epididymis was placed in 1 ml Embryo-max HTF media (Milipore-sigma, MR-070-D) pre-warmed to 37°C for 15 minutes. For counting, sperm were diluted in sterile water and counted using 5 fields of a hemocytometer. For motility, sperm were placed on a slide under a cover slip and 200 sperm were counted and characterized as motile or non-motile. Counts were performed in triplicates for each sample.

Tissue processing, immunogold labeling and electron microscopy. Anterior pituitary glands were cut into halves using a scalpel blade. Both halves were fixed by immersion for 3 h at room temperature with one half in 3% paraformaldehyde/0.05% glutaraldehyde in 0.1 M phosphate buffer (pH 7.2) for immunogold labeling, the other half in 2% paraformaldehyde/2.5% glutaraldehyde in 0.1 M phosphate buffer (pH 7.2) for 3 h at room temperature for optimal cell ultrastructure imaging. Protocols for immunogold labeling and optimal cell structure imaging are detailed in *Supplementary Methods*.

Primer sequences. See supplemental Table 1.

Antibodies and immuno-staining conditions. See supplemental Table 2.

Statistics. For all quantitative comparisons, data are presented as mean ± SD. For comparisons between 2 groups, statistical significance was determined using the 2-tailed Student's *t* test. For comparisons between multiple groups, homogeneity of variance between groups was determined by Brown-Forsythe test. For multiple groups that meet the homogeneity of variances assumption, one-way ANOVA was used to determine overall statistical significance, followed by the Student-

Newman-Keuls (SNK) post hoc test to determine significance between groups. A P value of less than 0.005 was considered statistically significant. Asterisks indicated statistical significance according to this legend: *P<0.05: **P<0.01; ***P<0.001; ****P<0.0001.

Study approval. Animals were maintained according to the National Institute of Health Guide for the Care and Use of Experimental Animals and with the approval from the Institutional Animal Care and Use Committee (IACUC) at Baylor College of Medicine.

Author Contributions

YAR conceived the project, designed and performed most of the experiments, analyzed and interpreted data, and wrote the manuscript. TM conceived, designed and performed the experiments with ovary and pituitary tissues, analyzed and interpreted the corresponding data, and wrote the manuscript. MTL and DJB designed experiments and interpreted data. HCC performed, analyzed, and interpreted pituitary transmission electron microscopy. CJJ and JAM performed, analyzed and interpreted studies with male reproductive tissues. JDL, SS, ISK and X H.-F. Z designed, analyzed and interpreted flow cytometry experiments. HMC contributed to immuno-staining and qPCR analyses. WC, YX, KJP and JH designed experiments and interpreted data of adipose tissues. HM and RAW contributed to the design of ovariectomy experiment and analysis of hypothalamus tissues. CL performed, analyzed and interpreted RNA *in situ* hybridization experiments. SP performed and analyzed mouse body composition studies. TFC contributed to the design of experiments involving FS cells. JSR contributed to experimental design and data interpretation, and wrote the manuscript. All authors read, edited, and approved the manuscript.

Acknowledgements

The authors thank Robert G. Cowan (Cornell University, Ithaca, NY, USA) for statistical analysis; Alan J. Conley (University of California at Davis, USA) for the CYP17A1 antibody; Martin J. Cohn (University of Florida, Gainesville, FL, USA) for providing the testis of *Ptch1*-LacZ mice; the Core facilities at Baylor College of Medicine, including the Breast Center Pathology Core, the RNA in situ Hybridization Core, the Optical Imaging & Vital microscopy Core, the Cytometry and Cell Sorting Core, the Mouse Metabolism and Phenotyping Core (R01DK114356 and UM1HG006348), the Integrated Microscopy Core and Pathology & Histology Core. The authors also thank the University of Virginia Center for Research in Reproduction Ligand Assay and Analysis Core,

644 which is supported by the Eunice Kennedy Shriver NICHD/NIH (NCTRI) Grant P50-HD28934.
645 This work was supported by Canadian Institutes of Health Research (CIHR) MOP-123447 (to
646 DJB), National Institute of Health (NIH) NIH-HD0076980 (to JSR), T32 HD007165 (supported
647 YAR); NIH-R01 CA-127857 (to MTL); National Science Foundation (NSF) NSF-1263742 (to MTL),
648 and NIH S10OD016167 (to MCL). RAW is supported by USDA/ARS CRIS 3092-5-001-059.

649

650

651

Reference

1. Monkkonen T, and Lewis MT. New paradigms for the Hedgehog signaling network in mammary gland development and breast Cancer. *Biochim Biophys Acta.* 2017;1868(1):315-32.
2. Ren Y, Cowan RG, Migone FF, and Quirk SM. Overactivation of hedgehog signaling alters development of the ovarian vasculature in mice. *Biol Reprod.* 2012;86(6):174.
3. Ren Y, Cowan RG, Harman RM, and Quirk SM. Dominant activation of the hedgehog signaling pathway in the ovary alters theca development and prevents ovulation. *Mol Endocrinol.* 2009;23(5):711-23.
4. Wijgerde M, Ooms M, Hoogerbrugge JW, and Grootegoed JA. Hedgehog signaling in mouse ovary: Indian hedgehog and desert hedgehog from granulosa cells induce target gene expression in developing theca cells. *Endocrinology.* 2005;146(8):3558-66.
5. Liu C, Peng J, Matzuk MM, and Yao HH. Lineage specification of ovarian theca cells requires multicellular interactions via oocyte and granulosa cells. *Nat Commun.* 2015;6:6934.
6. Yao HH, Whoriskey W, and Capel B. Desert Hedgehog/Patched 1 signaling specifies fetal Leydig cell fate in testis organogenesis. *Genes Dev.* 2002;16(11):1433-40.
7. Treier M, O'Connell S, Gleiberman A, Price J, Szeto DP, Burgess R, et al. Hedgehog signaling is required for pituitary gland development. *Development.* 2001;128(3):377-86.
8. Flemming GM, Klammt J, Ambler G, Bao Y, Blum WF, Cowell C, et al. Functional characterization of a heterozygous GLI2 missense mutation in patients with multiple pituitary hormone deficiency. *J Clin Endocrinol Metab.* 2013;98(3):E567-75.
9. Lampichler K, Ferrer P, Vila G, Lutz MI, Wolf F, Knosp E, et al. The role of proto-oncogene GLI1 in pituitary adenoma formation and cell survival regulation. *Endocr Relat Cancer.* 2015;22(5):793-803.
10. King PJ, Guasti L, and Laufer E. Hedgehog signalling in endocrine development and disease. *J Endocrinol.* 2008;198(3):439-50.
11. Le Tissier P, Fiordelisio Coll T, and Mollard P. The Processes of Anterior Pituitary Hormone Pulse Generation. *Endocrinology.* 2018;159(10):3524-35.
12. Mollard P, Hodson DJ, Lafont C, Rizzoti K, and Drouin J. A tridimensional view of pituitary development and function. *Trends Endocrinol Metab.* 2012;23(6):261-9.
13. Shimon I, Yan X, Ray DW, and Melmed S. Cytokine-dependent gp130 receptor subunit regulates human fetal pituitary adrenocorticotropin hormone and growth hormone secretion. *J Clin Invest.* 1997;100(2):357-63.
14. Akita S, Webster J, Ren SG, Takino H, Said J, Zand O, et al. Human and murine pituitary expression of leukemia inhibitory factor. Novel intrapituitary regulation of adrenocorticotropin hormone synthesis and secretion. *J Clin Invest.* 1995;95(3):1288-98.
15. Le Tissier P, Campos P, Lafont C, Romano N, Hodson DJ, and Mollard P. An updated view of hypothalamic-vascular-pituitary unit function and plasticity. *Nat Rev Endocrinol.* 2017;13(5):257-67.
16. Briscoe J, and Therond PP. The mechanisms of Hedgehog signalling and its roles in development and disease. *Nat Rev Mol Cell Biol.* 2013;14(7):416-29.
17. Allen BL, Song JY, Izzi L, Althaus IW, Kang JS, Charron F, et al. Overlapping roles and collective requirement for the coreceptors GAS1, CDO, and BOC in SHH pathway function. *Dev Cell.* 2011;20(6):775-87.
18. Bae GU, Domene S, Roessler E, Schachter K, Kang JS, Muenke M, et al. Mutations in CDON, encoding a hedgehog receptor, result in holoprosencephaly and defective interactions with other hedgehog receptors. *Am J Hum Genet.* 2011;89(2):231-40.
19. Finco I, LaPensee CR, Krill KT, and Hammer GD. Hedgehog signaling and steroidogenesis. *Annu Rev Physiol.* 2015;77:105-29.

20. Gross SR, Sin CG, Barraclough R, and Rudland PS. Joining S100 proteins and migration: for better or for worse, in sickness and in health. *Cell Mol Life Sci.* 2014;71(9):1551-79.
21. Lukanidin E, and Sleeman JP. Building the niche: the role of the S100 proteins in metastatic growth. *Semin Cancer Biol.* 2012;22(3):216-25.
22. Monkkonen T, Landua JD, Visbal AP, and Lewis MT. Epithelial and non-epithelial Ptch1 play opposing roles to regulate proliferation and morphogenesis of the mouse mammary gland. *Development.* 2017;144(7):1317-27.
23. Moraes RC, Chang H, Harrington N, Landua JD, Prigge JT, Lane TF, et al. Ptch1 is required locally for mammary gland morphogenesis and systemically for ductal elongation. *Development.* 2009;136(9):1423-32.
24. Wu R, Van der Hoek KH, Ryan NK, Norman RJ, and Robker RL. Macrophage contributions to ovarian function. *Hum Reprod Update.* 2004;10(2):119-33.
25. Brannstrom M, and Enskog A. Leukocyte networks and ovulation. *J Reprod Immunol.* 2002;57(1-2):47-60.
26. Bukulmez O, and Arici A. Leukocytes in ovarian function. *Hum Reprod Update.* 2000;6(1):1-15.
27. Bhowmick NA, Chytil A, Plieth D, Gorska AE, Dumont N, Shappell S, et al. TGF-beta signaling in fibroblasts modulates the oncogenic potential of adjacent epithelia. *Science.* 2004;303(5659):848-51.
28. DeFalco T, Potter Sarah J, Williams Alyna V, Waller B, Kan Matthew J, and Capel B. Macrophages Contribute to the Spermatogonial Niche in the Adult Testis. *Cell Reports.* 2015;12(7):1107-19.
29. Gergics P, Christian HC, Choo MS, Ajmal A, and Camper SA. Gene Expression in Mouse Thyrotrope Adenoma: Transcription Elongation Factor Stimulates Proliferation. *Endocrinology.* 2016;157(9):3631-46.
30. Barash IA, Cheung CC, Weigle DS, Ren H, Kabigting EB, Kuijper JL, et al. Leptin is a metabolic signal to the reproductive system. *Endocrinology.* 1996;137(7):3144-7.
31. Chen W, Chang B, Saha P, Hartig SM, Li L, Reddy VT, et al. Berardinelli-seip congenital lipodystrophy 2/seipin is a cell-autonomous regulator of lipolysis essential for adipocyte differentiation. *Mol Cell Biol.* 2012;32(6):1099-111.
32. Chen W, Zhou H, Saha P, Li L, and Chan L. Molecular mechanisms underlying fasting modulated liver insulin sensitivity and metabolism in male lipodystrophic Bscl2/Seipin-deficient mice. *Endocrinology.* 2014;155(11):4215-25.
33. Allaerts W, Jeucken PH, Bosman FT, and Drexhage HA. Relationship between dendritic cells and folliculo-stellate cells in the pituitary: immunohistochemical comparison between mouse, rat and human pituitaries. *Adv Exp Med Biol.* 1993;329:637-42.
34. Allaerts W, Jeucken PH, Hofland LJ, and Drexhage HA. Morphological, immunohistochemical and functional homologies between pituitary folliculo-stellate cells and lymphoid dendritic cells. *Acta Endocrinol (Copenh).* 1991;125 Suppl 1:92-7.
35. Inoue K, Couch EF, Takano K, and Ogawa S. The structure and function of folliculo-stellate cells in the anterior pituitary gland. *Arch Histol Cytol.* 1999;62(3):205-18.
36. Fauquier T, Guerineau NC, McKinney RA, Bauer K, and Mollard P. Folliculostellate cell network: a route for long-distance communication in the anterior pituitary. *Proc Natl Acad Sci U S A.* 2001;98(15):8891-6.
37. Golan M, Hollander-Cohen L, and Levavi-Sivan B. Stellate Cell Networks in the Teleost Pituitary. *Sci Rep.* 2016;6:24426.
38. Wynn TA, Chawla A, and Pollard JW. Macrophage biology in development, homeostasis and disease. *Nature.* 2013;496(7446):445-55.
39. Christian JMaH. Folliculo-stellate cells: paracrine communicators in the anterior pituitary. *The Open Neuroendocrinology Journal.* 2011;4:77-89.

40. Baes M, Allaerts W, and Denef C. Evidence for functional communication between folliculo-stellate cells and hormone-secreting cells in perifused anterior pituitary cell aggregates. *Endocrinology.* 1987;120(2):685-91.
41. Wu R, Fujii S, Ryan NK, Van der Hoek KH, Jasper MJ, Sini I, et al. Ovarian leukocyte distribution and cytokine/chemokine mRNA expression in follicular fluid cells in women with polycystic ovary syndrome. *Hum Reprod.* 2007;22(2):527-35.
42. Kozlova FAaEN. Metastasis-associated Mts1 (S100A4) protein in the development and adult central nervous system. *The Journal of Comparative Neurology.* 2000;424:269-82.
43. Horiguchi K, Fujiwara K, Yoshida S, Higuchi M, Tsukada T, Kanno N, et al. Isolation of dendritic-cell-like S100beta-positive cells in rat anterior pituitary gland. *Cell Tissue Res.* 2014;357(1):301-8.
44. Crompton T, Outram SV, and Hager-Theodorides AL. Sonic hedgehog signalling in T-cell development and activation. *Nat Rev Immunol.* 2007;7(9):726-35.
45. Furmanski AL, Saldana JI, Ono M, Sahni H, Paschalidis N, D'Acquisto F, et al. Tissue-derived hedgehog proteins modulate Th differentiation and disease. *J Immunol.* 2013;190(6):2641-9.
46. Dierks C, Grbic J, Zirlik K, Beigi R, Englund NP, Guo GR, et al. Essential role of stromally induced hedgehog signaling in B-cell malignancies. *Nat Med.* 2007;13(8):944-51.
47. Vila G, Theodoropoulou M, Stalla J, Tonn JC, Losa M, Renner U, et al. Expression and function of sonic hedgehog pathway components in pituitary adenomas: evidence for a direct role in hormone secretion and cell proliferation. *J Clin Endocrinol Metab.* 2005;90(12):6687-94.
48. Vila G, Papazoglou M, Stalla J, Theodoropoulou M, Stalla GK, Holsboer F, et al. Sonic hedgehog regulates CRH signal transduction in the adult pituitary. *FASEB J.* 2005;19(2):281-3.
49. Franca MM, Jorge AA, Carvalho LR, Costalonga EF, Vasques GA, Leite CC, et al. Novel heterozygous nonsense GLI2 mutations in patients with hypopituitarism and ectopic posterior pituitary lobe without holoprosencephaly. *J Clin Endocrinol Metab.* 2010;95(11):E384-91.
50. Fang Q, George AS, Brinkmeier ML, Mortensen AH, Gergics P, Cheung LY, et al. Genetics of Combined Pituitary Hormone Deficiency: Roadmap into the Genome Era. *Endocr Rev.* 2016;37(6):636-75.
51. Kendall SK, Samuelson LC, Saunders TL, Wood RI, and Camper SA. Targeted disruption of the pituitary glycoprotein hormone alpha-subunit produces hypogonadal and hypothyroid mice. *Genes Dev.* 1995;9(16):2007-19.
52. Cao D, Ma X, Cai J, Luan J, Liu AJ, Yang R, et al. ZBTB20 is required for anterior pituitary development and lactotrope specification. *Nat Commun.* 2016;7:11121.
53. Jung DO, Jasurda JS, Egashira N, and Ellsworth BS. The forkhead transcription factor, FOXP3, is required for normal pituitary gonadotropin expression in mice. *Biol Reprod.* 2012;86(5):144, 1-9.
54. Bonnefont X, Lacampagne A, Sanchez-Hormigo A, Fino E, Creff A, Mathieu MN, et al. Revealing the large-scale network organization of growth hormone-secreting cells. *Proc Natl Acad Sci U S A.* 2005;102(46):16880-5.
55. Sanchez-Cardenas C, Fontanaud P, He Z, Lafont C, Meunier AC, Schaeffer M, et al. Pituitary growth hormone network responses are sexually dimorphic and regulated by gonadal steroids in adulthood. *Proc Natl Acad Sci U S A.* 2010;107(50):21878-83.
56. Alim Z, Hartshorn C, Mai O, Stitt I, Clay C, Tobet S, et al. Gonadotrope plasticity at cellular and population levels. *Endocrinology.* 2012;153(10):4729-39.
57. Bianco SD, and Kaiser UB. The genetic and molecular basis of idiopathic hypogonadotropic hypogonadism. *Nat Rev Endocrinol.* 2009;5(10):569-76.

58. Fraietta R, Zylberstejn DS, and Esteves SC. Hypogonadotropic hypogonadism revisited. *Clinics (Sao Paulo).* 2013;68 Suppl 1:81-8.
59. Allaerts W, and Vankelecom H. History and perspectives of pituitary folliculo-stellate cell research. *Eur J Endocrinol.* 2005;153(1):1-12.
60. Jasper MJ, Tremellen KP, and Robertson SA. Primary unexplained infertility is associated with reduced expression of the T-regulatory cell transcription factor Foxp3 in endometrial tissue. *Mol Hum Reprod.* 2006;12(5):301-8.
61. Hori S, Nomura T, and Sakaguchi S. Control of regulatory T cell development by the transcription factor Foxp3. *Science.* 2003;299(5609):1057-61.
62. Lahl K, Loddenkemper C, Drouin C, Freyer J, Arnason J, Eberl G, et al. Selective depletion of Foxp3+ regulatory T cells induces a scurfy-like disease. *J Exp Med.* 2007;204(1):57-63.
63. Ellis T, Smyth I, Riley E, Graham S, Elliot K, Narang M, et al. Patched 1 conditional null allele in mice. *Genesis.* 2003;36(3):158-61.
64. Goodrich LV, Milenkovic L, Higgins KM, and Scott MP. Altered neural cell fates and medulloblastoma in mouse patched mutants. *Science.* 1997;277(5329):1109-13.
65. Liu Z, Castrillon DH, Zhou W, and Richards JS. FOXO1/3 depletion in granulosa cells alters follicle growth, death and regulation of pituitary FSH. *Mol Endocrinol.* 2013;27(2):238-52.

Figure 1.

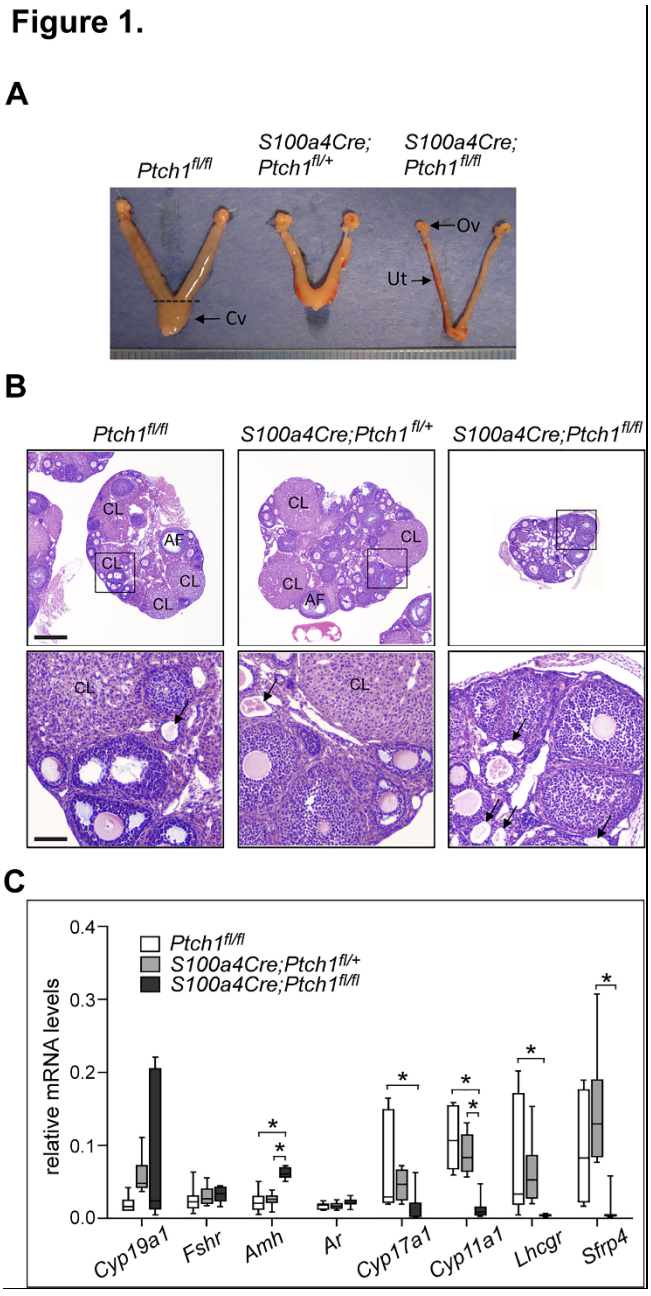

Figure 1. Homozygous ablation of *Ptch1* with *S100a4-Cre* leads to hypogonadism in female mice. (**A**) Representative images of wild-type control, heterozygous, and homozygous *Ptch1* mutant mouse ovaries (Ov) and uteri (Ut) morphology, as well as (**B**) ovary histology with H&E staining. Cv: cervix. Scale bars: 400 μm (lower-magnification images, upper panels and 80 μm (higher-magnification images, lower panels). CL, corpus luteum; AF, antral follicle; arrows: degenerating oocyte. (**C**) Relative mRNA levels of ovarian function genes in whole ovaries from wild-type control, heterozygous, and homozygous *Ptch1* mutants (n=7). Total RNA was assayed by qPCR and the concentration of each transcript was normalized to that of housekeeping gene *Rpl19*. All data are from mice at 8 weeks of age and represented as mean ± SD. **P*<0.05; one-way ANOVA followed by SNK post hoc test.

Figure 2.

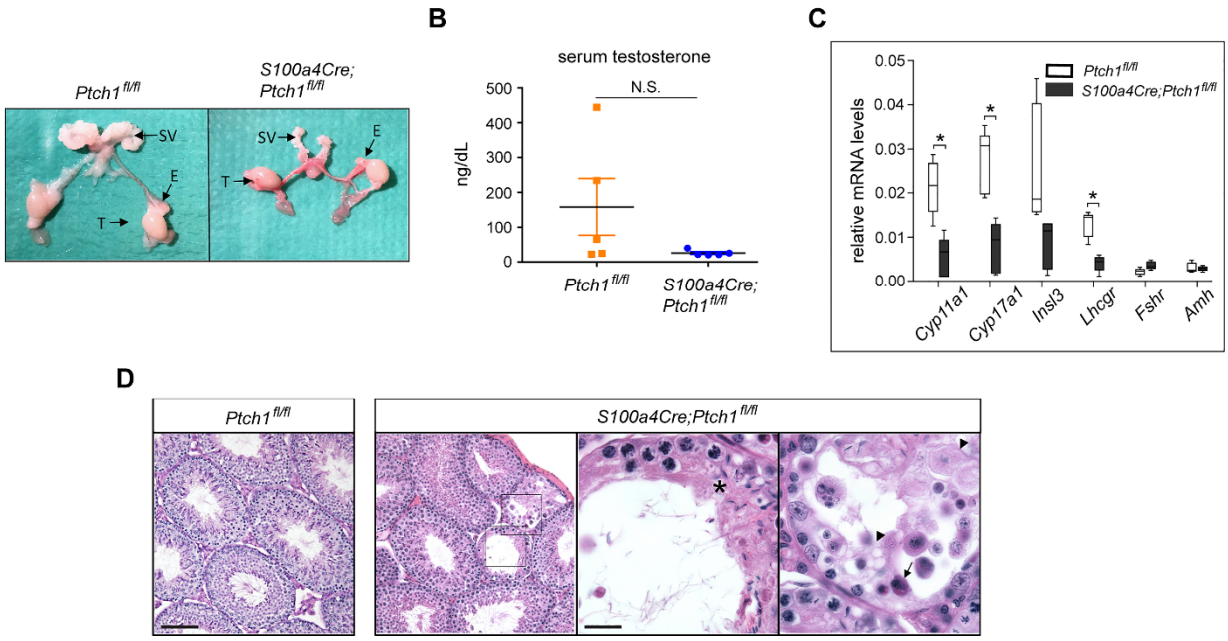

Figure 2. Homozygous ablation of *Ptch1* with *S100a4-Cre* leads to hypogonadism in male mice. (**A**) Representative images of wild-type control and homozygous *Ptch1* mutant male reproductive tissue morphology, including seminal vesicles (SV), epididymis (E) and testes (T). (**B**) Serum concentration of testosterone in control and homozygous *Ptch1* mutant male mice (n=5). (**C**) Relative mRNA levels of testis function genes in whole testes from wild-type control and homozygous *Ptch1* mutants (n=5). Total RNA was assayed by qPCR and the concentration of each transcript was normalized to that of housekeeping gene *Rpl19*. Data are represented as mean ± SD. **P*<0.05; *t* test. (**D**) Representative images of wild-type control and homozygous *Ptch1* mutant seminiferous tubules with PAS staining. Scale bars: 100 μm (lower-magnification images) and 25 μm (higher-magnification images). Asterisk: impaired hierarchical organization; arrow: multinucleated cells; arrowheads: vacuoles. All data are from mice at 8 weeks of age.

Table 1.

Female parameters	28 day (n=4)		56 day (n=6)	
	WT	KO	WT	KO
Body (g)	14.49 ± 0.65	14.22 ± 0.70	24.12 ± 1.16	15.47 ± 1.18****
ovary (mg)	1.11 ± 0.06	1.13 ± 0.01	4.48 ± 0.54	1.18 ± 0.10****
% ovary/body weight	0.77 ± 0.06	0.79 ± 0.11	1.86 ± 0.26	0.77 ± 0.07****
uterus (mg)	6.26 ± 0.53	6.73 ± 0.66	27.82 ± 6.52	5.34 ± 0.50***
% uterus/body weight	4.32 ± 0.29	4.64 ± 0.53	11.38 ± 3.57	3.43 ± 0.28**

Table 2.

Male parameters	30 day		48 day	
	WT (n=4)	KO (n=4)	WT (n=8)	KO (n=9)
Body (g)	19.23 ± 1.46	18.10 ± 1.01	23.56 ± 2.61	16.64 ± 0.96****
Testis (mg)	61.50 ± 6.59	61.94 ± 8.45	95.57 ± 12.84	75.48 ± 6.46***
% testis/body weight	0.32 ± 0.02	0.34 ± 0.04	0.42 ± 0.01	0.45 ± 0.05
Epididymis (mg)	22.43 ± 5.36	19.06 ± 4.45	35.01 ± 4.37	25.34 ± 8.36**
% Epididymis/body weight	0.12 ± 0.02	0.11 ± 0.03	0.15 ± 0.03	0.14 ± 0.05
Seminal Vesicles (mg)	n/a	n/a	162.74 ± 40.10	60.55 ± 21.26****
% Seminal Vesicles/body weight	n/a	n/a	0.68 ± 0.14	0.36 ± 0.12**
Sperm Count (x10^6)	n/a	n/a	23.61 ± 3.70	6.97 ± 3.17****
Sperm Motility (%)	n/a	n/a	32.38 ± 9.49	5.86 ± 6.36****

Figure 3.

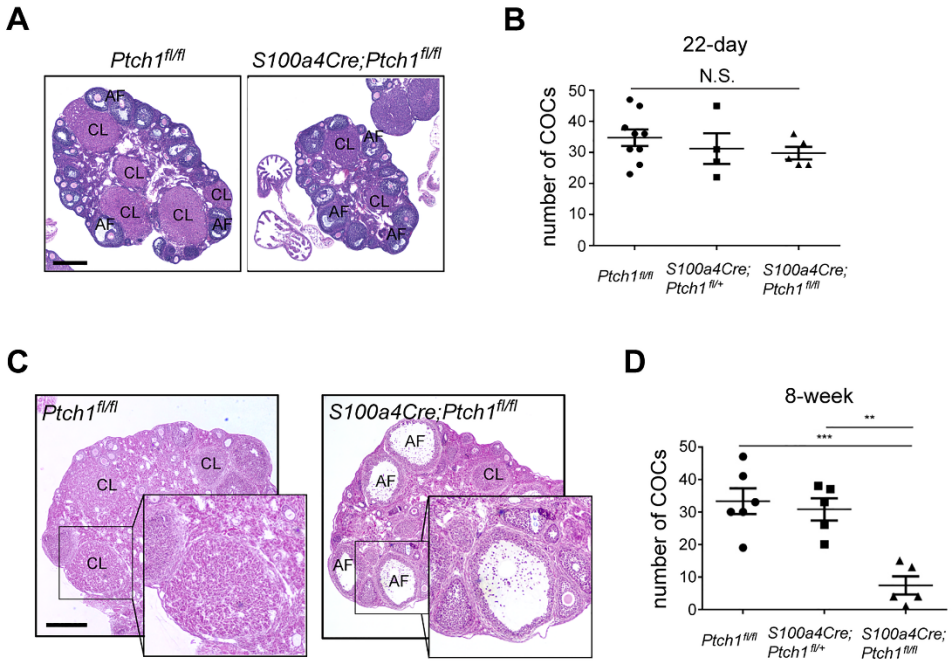

Figure 3. Hypogonadism in *Ptch1* mutant mice develops during the puberty to adult transition. (**A**) Representative images of wild-type control and homozygous *Ptch1* mutant female ovarian histology with H&E staining at 5 weeks of age. CL, corpus luteum; AF, antral follicles. Scale bar: 400 μm. (**B**) Numbers of cumulus-oocyte-complexes (COCs) ovulated into the oviduct and counted at 20 hours post-hCG during a superovulation stimulation in wild-type control, heterozygous and homozygous *Ptch1* mutant females at 22 days of age (n=9, wild-type; n=4, heterozygous mutant; and n=5, homozygous mutant). (**C**) Representative images of wild-type control and homozygous *Ptch1* mutant female ovarian histology with H&E staining at 8 weeks of age with superovulation stimulation (20 hours post-hCG). Scale bar: 400 μm. (**D**) Numbers of COCs ovulated into the oviduct and counted at 20 hours post-hCG during a superovulation stimulation in wild-type control, heterozygous, and homozygous *Ptch1* mutant females at 8 weeks of age (n=6, wild-type; n=5, heterozygous mutant; and n=5, homozygous mutant). ***P*<0.01; ****P*<0.001; one-way ANOVA followed by SNK post hoc test.

Figure 4.

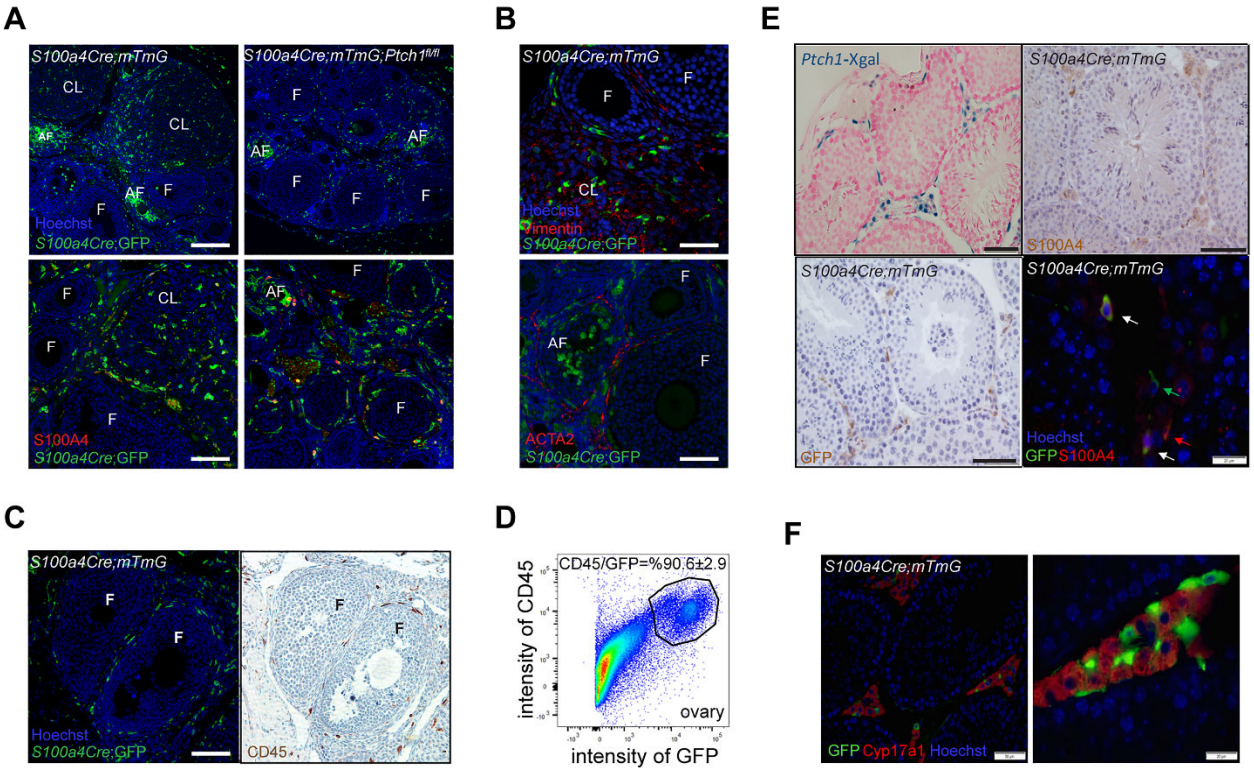

Figure 4. *S100a4-Cre* is expressed in CD45^{+} cells in the gonads. (**A**) Representative images of IF staining of GFP and S100A4 in the ovaries of reporter controls and homozygous *Ptch1* mutants (both express GFP driven by *S100a4-Cre*). CL, corpus luteum; F, follicles; AF, atretic follicles. Scale bars: 200 μm (upper panels) and 100 μm (lower panels). (**B**) Representative images of IF staining of GFP with vimentin or ACTA2 in the ovaries of reporter controls and homozygous *Ptch1* mutants. Scale bars: 40 μm (upper panels) and 75 μm (lower panels). (**C**) Representative images of IF staining of GFP and IHC staining of CD45 on adjacent serial sections of ovaries from reporter controls and homozygous *Ptch1* mutants. Scale bar: 100 μm. (**D**) The percentage of CD45-positive cells among GFP-positive cells in the ovaries of *S100a4-Cre;mTmG* reporter control mice analyzed by flow cytometry. The image represents results from three independent samples each of which contained dispersed ovarian cells pooled from 4 females. (**E**) Representative images of Xgal signal in testes of *Ptch1*-Xgal mice, as well as S100a4 and GFP staining in the testis of *S100a4-Cre;mTmG* reporter control mice. Arrows point to cells positive for GFP alone (green), S100A4 alone (red), or for both GFP and S100A4 (white). Scale bars: 50 μm and 20 μm. (**F**) Representative images of IF staining of GFP and CYP17A1 in testes of *S100a4-Cre;mTmG* reporter control mice. The right panel is a zoomed in view of the same tissue and staining as the left panel. Scale bars: 50 μm (left image) and 20 μm (right image).

Figure 5.

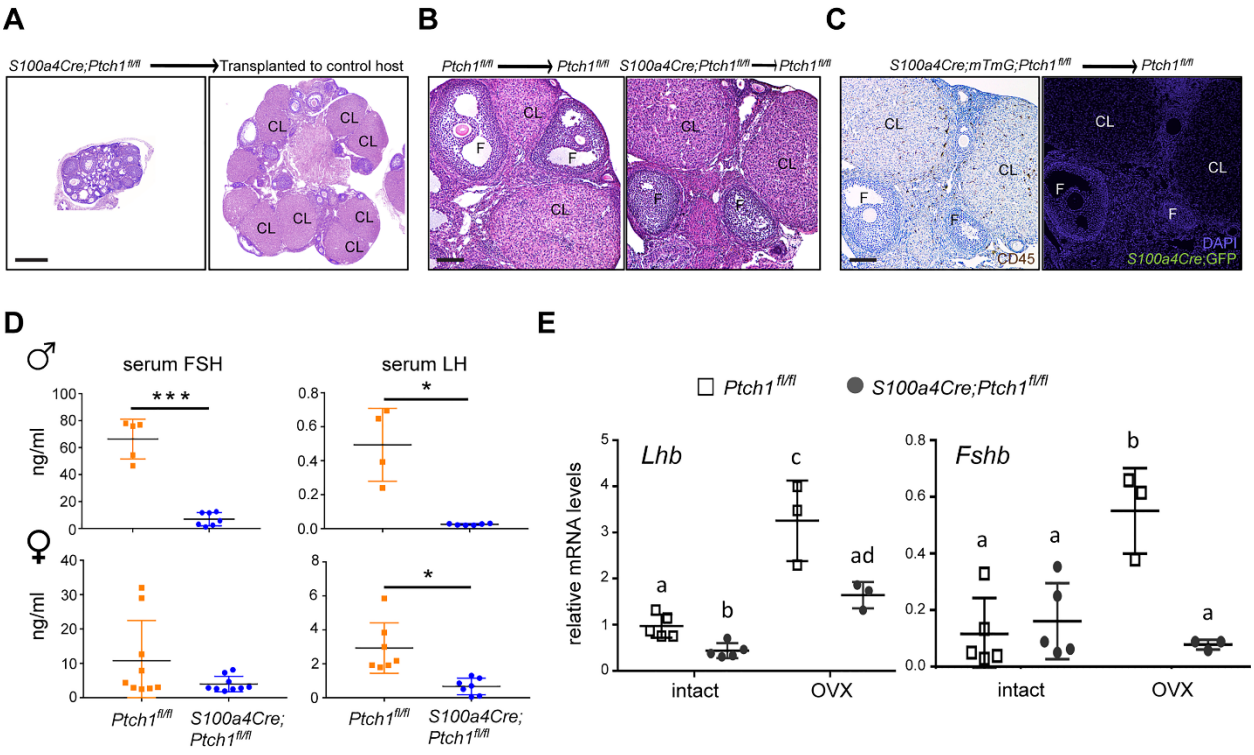

Figure 5. Gonad-extrinsic factors contribute to hypogonadism in Ptch1 mutant mice. (**A**) Representative images of ovaries of *S100a4-Cre;Ptch1$^{fl/fl}$;mTmG* mutant mice *in situ* (left) or transplanted to the bursa of control littermates (*Ptch1$^{fl/fl}$*) for 4 weeks (right). CL, corpus luteum; F, follicles. Scale bar: 200 μm. (**B**) Representative images of ovaries of *Ptch1$^{fl/fl}$* control mice (left) and *S100a4-Cre;Ptch1$^{fl/fl}$;mTmG* mutant mice (right) transplanted to control littermates (*Ptch1$^{fl/fl}$*) for 4 weeks. Scale bar: 100 μm. (**C**) Representative images of IHC staining of CD45 and IF staining of GFP on adjacent serial sections of ovaries from *S100a4-Cre;Ptch1$^{fl/fl}$;mTmG* mutant mice transplanted to *Ptch1$^{fl/fl}$* control mice. Scale bar: 100 μm. (**D**) Serum concentration of FSH and LH in control and homozygous *Ptch1* mutant male and female mice at 8 weeks of age. *P<0.05; ***P<0.001; *t* test. (**E**) Relative mRNA levels of pituitary *Lhb* and *Fshb* in wild-type controls and homozygous *Ptch1* mutants with and without ovariectomy (OVX) (n= 3 for samples from OVX mice; n=5 for samples from intact mice). Total RNA was assayed by qPCR and the concentration of each transcript was normalized to that of housekeeping gene *Rpl19*. Data are represented as mean ± SD. Bars without common superscripts are significantly different (P<0.05); two-way ANOVA; All data are from mice at 8 weeks of age.

Figure 6.

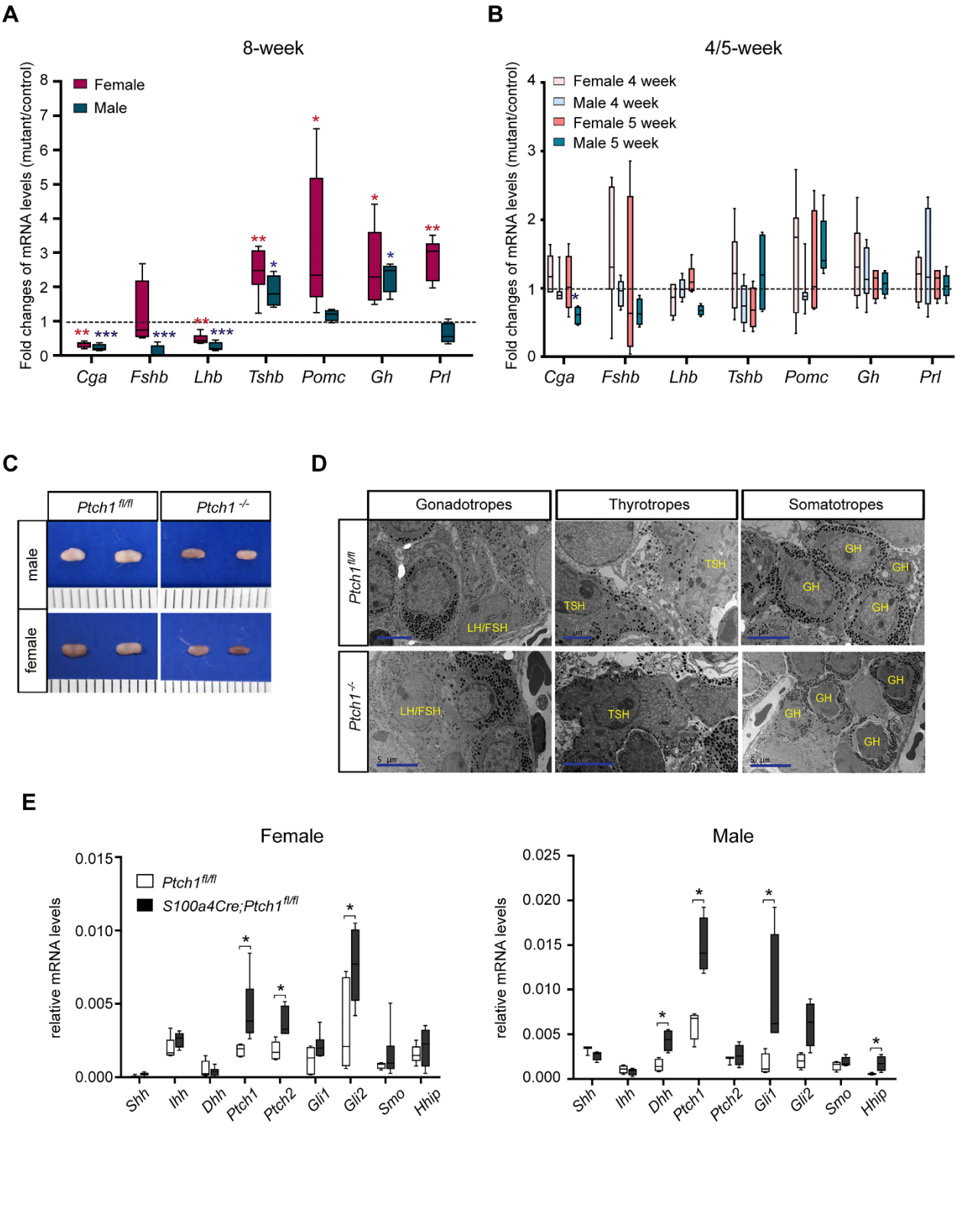
A
8-week
Female
Male
Fold changes of mRNA levels (mutant/control)
Cga
Fshb
Lhb
Tshb
Pomc
Gh
Prl
B
4/5-week
Female 4 week
Male 4 week
Female 5 week
Male 5 week
C
Ptch1 fl/fl
Ptch1 -/-
male
female
D
Gonadotropes
Thyrotropes
Somatotropes
LH/FSH
TSH
GH
E
Female
Male
Ptch1 fl/fl
S100a4Cre;Ptch1 fl/fl
relative mRNA levels
Shh
Ihh
Dhh
Ptch1
Ptch2
Gli1
Gli2
Smo
Hhip

Figure 6. Adult *Ptch1* mutant mice exhibit severe pituitary abnormalities with sexually dimorphic manifestation. Relative mRNA levels of pituitary endocrine function genes in whole pituitaries of wild-type controls and homozygous *Ptch1* mutants at 8 weeks (**A**), 4 weeks (**B**, bars of lighter pink and blue colors), and 5 weeks (**B**, bars of darker pink and blue colors) of age (**B**). Total RNA was assayed by qPCR and the concentration of each transcript was normalized to that of housekeeping gene *Rpl19*. Data are presented as fold change of mRNA levels in mutants versus wild-type controls (n≥ 5). **P*<0.05; ***P*<0.01; *t* test. (**C**) Representative images of pituitary morphology at 8 weeks of age. Scale is in units of millimeters. (**D**) Representative images of transmission electron microscopy on pituitary tissues from control and *Ptch1* mutant mice at 8 weeks of age. Endocrine cell types are identified according to their ultra-structural features and labeled with the name of the hormones they produce. The images of gonadotropes are from male mice; and the images of thyrotropes and somatotropes are from female mice. Scale bars: 5 μm and 2 μm. (**E**) Relative mRNA levels of genes in the HH signaling pathway in whole pituitary tissues of wild-type controls and homozygous *Ptch1* mutants at 8 weeks of age (n≥ 5). Total RNA was assayed by qPCR and the concentration of each transcript was normalized to that of housekeeping gene *Rpl19*. Data are represented as mean ± SD. **P*<0.05; *t* test.

Figure 7.

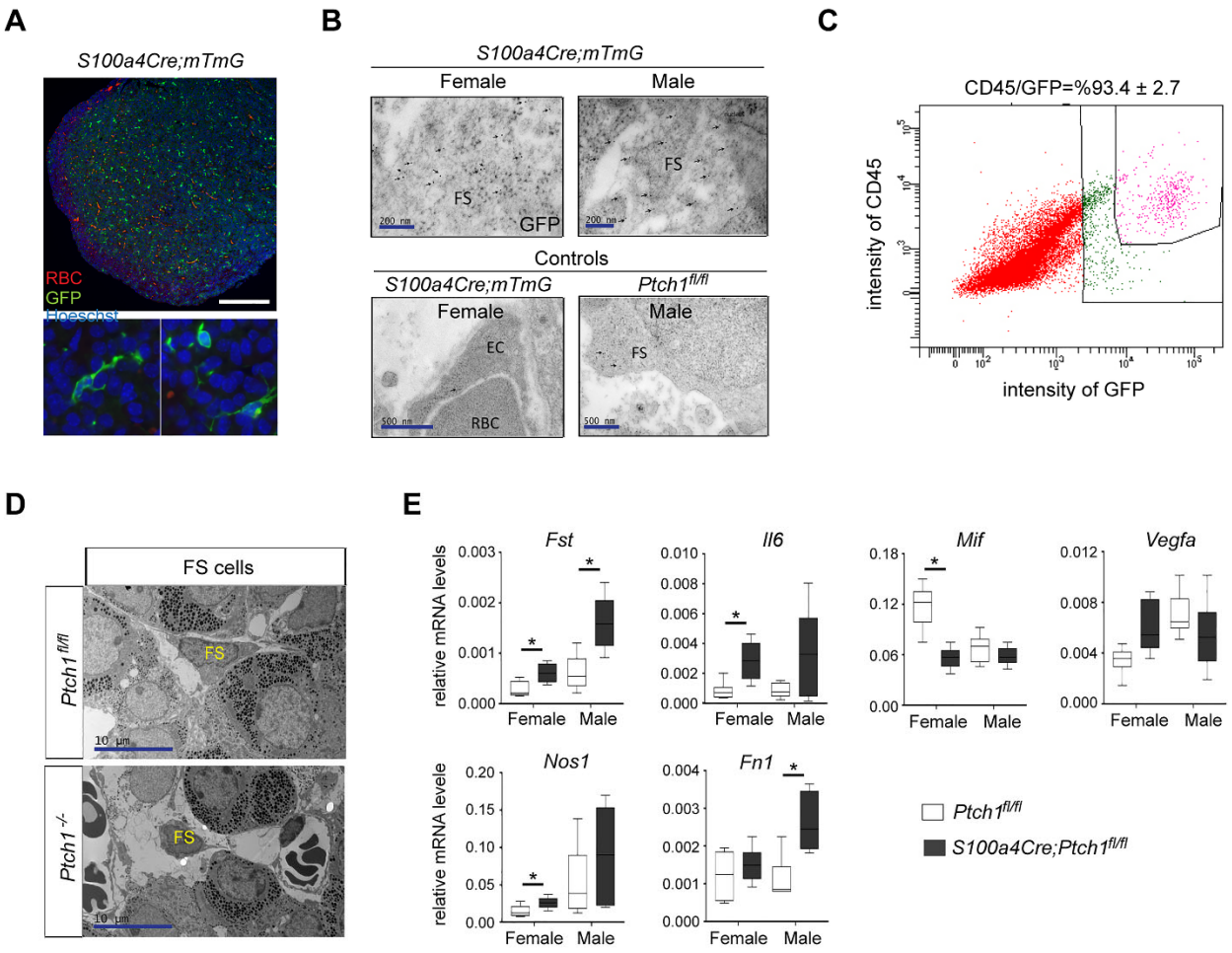

Figure 7. Expression of *S100a4-Cre* is restricted to CD45⁺ cells, including FS cells, in the anterior pituitary and leads to malfunction of these cells. (**A**) Representative images of IF staining for GFP in the anterior pituitary of *S100a4-Cre;mTmG* reporter control mice. RBC: red blood cell. Scale bars: 200 µm and 20 µm. (**B**) Representative images of transmission electron microscopy of immunogold labeling of GFP on pituitary tissue sections from *S100a4-Cre;mTmG* reporter mice at 8 weeks of age. Arrows point to immunogold signals. FS, folliculo-stellate cells; EC, endothelial cells. Scale bars: 200 nm (top panels) and 500 nm (bottom panels). (**C**) The percentage of CD45-positive cells amount GFP-positive cells in the pituitaries of *S100a4-Cre;mTmG* reporter control mice analyzed by flow cytometry. The image represents results from four independent samples. (**D**) Representative images of transmission electron microscopy of FS cells in control and *Ptch1* mutant mice. FS cells are identified according to their ultra-structural features. Scale bar: 10 µm. (**E**) Relative mRNA levels of genes involved in the pituitary microenvironment in whole pituitary tissues of wild-type controls and homozygous *Ptch1* mutants at 8 weeks of age (n≥5). Total RNA was assayed by qPCR and the concentration of each

943 transcript was normalized to that of a housekeeping gene *Rpl19*. Data are represented as mean
944 ± SD. *P<0.05; *t* test. All data are from mice at 8 weeks of age.

945